Catalysis Today 154 (2010) 202–209

Contents lists available at ScienceDirect

Catalysis Today

journal homepage: www.elsevier.com/locate/cattod

Detailed kinetics of the Fischer–Tropsch synthesis over Co-based catalysts containing sulphur

Carlo Giorgio Visconti[a,1], Luca Lietti[a,*], Enrico Tronconi[a], Pio Forzatti[a], Roberto Zennaro[b], Stefano Rossini[c]

[a] Politecnico di Milano, Dipartimento di Energia, Piazza Leonardo da Vinci, 32- 20133 Milano, Italy
[b] Eni, Divisione Exploration & Production, Via Emilia, 1 - 20097 San Donato Milanese, Italy
[c] Eni, Divisione Refining & Marketing, Via Felice Maritano, 26 - 20097 San Donato Milanese, Italy

ARTICLE INFO

Article history:
Available online 14 May 2010

Keywords:
Fischer–Tropsch synthesis
Catalyst deactivation
Sulphur poisoning
Kinetics
Catalyst selectivity
Cobalt
Mathematical modeling
CO conversion
Product distribution

ABSTRACT

The effect of sulphur poisoning on the activity and selectivity in the Fischer–Tropsch synthesis of a Co/γ-Al_2O_3 catalyst, investigated in a previous work under conditions relevant to industrial operation, has been described in this work by means of a complete kinetic model, able to predict at the same time the CO conversion and the product distribution (paraffins and olefins from C_1 to C_{50}) on the basis of the process conditions and the amount of sulphur on the catalyst. To reach this goal, a mechanistic kinetic model, developed in a previous work for an unpoisoned catalyst, has been modified introducing the dependence on sulphur of the total number of catalytic active sites (to describe the progressive decrease of the catalyst activity with increasing sulphur loading on the catalyst), of the rate of the chain growth step (to describe the decrease of the selectivity to heavy products observed with sulphur-poisoned catalysts), and of the rates of paraffins and olefins formation from the growing adsorbed intermediate (to describe the variation of the olefin/paraffin ratio in the reaction products collected with the poisoned catalysts).

1. Introduction

The Fischer–Tropsch synthesis (FTS) is a surface catalyzed process discovered in 1923, in which the synthesis gas, the mixture of carbon monoxide and hydrogen, is converted into water, other oxygenates and hydrocarbons with a broad range of chain length and functionality [1]. In last decade, this process has received considerable attention by both the industrial and the academic worlds as a way of exploiting coal, biomasses or the huge and cheap natural gas reserves located in remote areas, leading to high-grade synthetic lubricating oils and high-added value fuels (diesel with an high cetane number, sulphur- and aromatic-free) [2,3].

The FTS can be schematically described as polymerizations process, in which CO and H_2 react to form a monomer, which then grows to form the reaction products according to the following lumped stoichiometry:

$$n\mathrm{CO} + 2n\mathrm{H_2} \rightarrow -(\mathrm{CH_2})_n + n\mathrm{H_2O} \quad (1)$$

The synthesis of the reaction products is strongly exothermic, releasing 165 kJ per each mole of converted CO. In general, the heavy paraffins (waxes) are the preferred products, since they can be easily hydrocracked to the so-called middle distillates, which represent the FT products with the highest added value.

Due to their cost, activity and selectivity, cobalt and iron are the most widely studied Fischer–Tropsch catalysts, and the only ones to be used at the industrial scale. The other metals active in the synthesis, namely nickel and ruthenium, have been used until now only as catalyst for research purposes or as promoters of cobalt and iron-based catalysts [4].

Like for many other catalysts, it is known that S-compounds contained in coal, biomasses or natural gas are effective poisons for Fischer–Tropsch catalysts [4–10]. It has been suggested that in order to minimize the deactivation of both iron and cobalt-based industrial Fischer–Tropsch catalysts, the sulphur content of syngas should be kept lower than 0.02 mg/m^3 [4]. Besides, alkali promoters are often added in order to limit the catalyst deactivation by sulphur [11].

In a previous work [5], we reported the results of an experimental investigation on the reactivity of a bench-scale Co/Al_2O_3 un-promoted catalyst, pre-poisoned with different amounts of sulphur (in the range 0–2000 ppm_w) according to an ex situ procedure (i.e. by impregnation) to overcome the experimental complexity associated to the use of S-carrier molecules. In this way, the poison concentration was a priori known and constant with the time on stream and the S-concentration gradients in the catalyst bed,

* Corresponding author. Tel.: +39 02 2399 3272; fax: +39 02 2399 3318.
E-mail address: luca.lietti@polimi.it (L. Lietti).
[1] http://www.lccp.polimi.it.

0920-5861/$ – see front matter © 2010 Elsevier B.V. All rights reserved.
doi:10.1016/j.cattod.2010.04.007

Table 1
Experimental CO conversion values for samples loaded with different amounts of sulphur (experimental conditions as in Fig. 1). Data are taken from Ref. [5].

Catalyst sample	Sulphur loading (ppm_w)	CO conversion (%)
S0	0	24.0
S10	10	18.8
S100	100	15.3
S250	250	9.4
S2000	2000	3.0

typical of fixed-bed reactors fed with a S-containing feed, could be safely neglected.

The feasibility of studying S-poisoning adopting a catalyst pre-poisoning procedure (ex situ poisoning) has been discussed in our previous work [5], detailing the possible differences between the ex situ and the in situ poisoning by S-compounds during the FTS. It has been shown that in situ poisoning with S-carrier molecules suffers of two main drawbacks: first, the low concentration which is required in the feed stream, associated with the high adsorption capability of S-carrier molecules (typically H_2S) in the rig lines, makes very difficult to precisely know the amount of sulphur reaching the catalyst samples; second, the high adsorption capability of H_2S on the catalyst may lead to the presence of intraparticle sulphur gradients in the catalyst pellets and, in the case of fixed-bed reactors, to the presence of axial S-concentration gradients in the catalyst bed, thus making very complex the kinetic analysis of experimental data obtained in the presence of sulphur.

An obvious issue of the pre-poisoning method is that the S-catalyst interactions may be different with that established under actual reaction conditions. The strategy followed to limit this drawback is discussed in [5]. Particular attention was given to the poisoning process that has been carried out on a pre-reduced catalyst to simulate the S–Co interactions under actual synthesis conditions.

From a morphological point of view, we observed the added sulphur does not lead to appreciable variations in the catalyst characteristics; on the contrary, sulphur decreased the catalyst reducibility by hydrogen, preventing the formation of the active phase in the FT process, namely the metallic cobalt.

Concerning the FT catalytic performances, the comparison between the product yields of samples loaded with different amounts of sulphur pointed out that the presence of this atom on the catalyst surface remarkably affects both the activity and the selectivity of the reaction.

The CO conversion data obtained running catalysts pre-loaded with different amounts of sulphur (0, 10, 100, 250 and 2000 ppm_w) at the same process conditions (220 °C, 20 bar, 2 mol_{H_2}/mol_{CO}, 5000 $cm^3(STP)_{CO+H_2}/h/g_{cat}$) are reported in Table 1, while the selectivity to the different reaction products is reported in Fig. 1 in terms of total hydrocarbons (a), n-paraffins (b) and α-olefins (c).

The addition of sulphur determines a progressive decrease of the CO conversion, so that the activity of heavier sulphured catalyst (2000 ppm) is almost completely compromised. Moreover, sulphur significantly changes the product distribution, decreasing the formation of heavier species (both C_{5+} and C_{25+}), thus driving the selectivity of the reaction towards light products, and changing the olefinicity of the products.

Notably, we found that the effects of sulphur very with the sulphur loading: indeed for low S amounts (<100 ppm) the CO conversion is decreased whereas the product distribution is not significantly affected; at higher S loadings a significant decrease in the formation of heavier products is observed along with a further decrease in CO conversion.

The experimental data of CO conversion decay with S-loading were also kinetically described in [5] in order to find a mathematical model able to predict the catalyst activity loss as a function of the sulphur content on the surface. A literature power-law expression ($r_{CO} = kP_{H_2}^{0.74}P_{CO}^{-0.24}$) [12] was used to describe the activity of the unpoisoned catalyst, while the CO conversion rates in the case of the sulphur-poisoned samples were described by introducing in the expression of the kinetic constant k a term depending on the sulphur content on the catalyst. It was found that the experimental results are nicely described by adopting a relationship with the following structure:

$$k = \frac{k^0}{(1+\alpha S)^m} \quad (2)$$

where k^0 is the kinetic constant of the unpoisoned catalyst sample, S the sulphur content on the catalyst expressed in mg_S/kg_{cat} and α, m two positive adaptive parameters estimated upon regression of the experimental data.

Such a model is extremely simple and for this reason can be easily applied to estimate the total productivity of lab- and bigger-scale reactors working with cobalt-based catalysts, fresh or partially poisoned with sulphur. However, it does not provide any information concerning the products distribution, which is well known to be a crucial aspect for the industrialization of the Fischer–Tropsch syn-

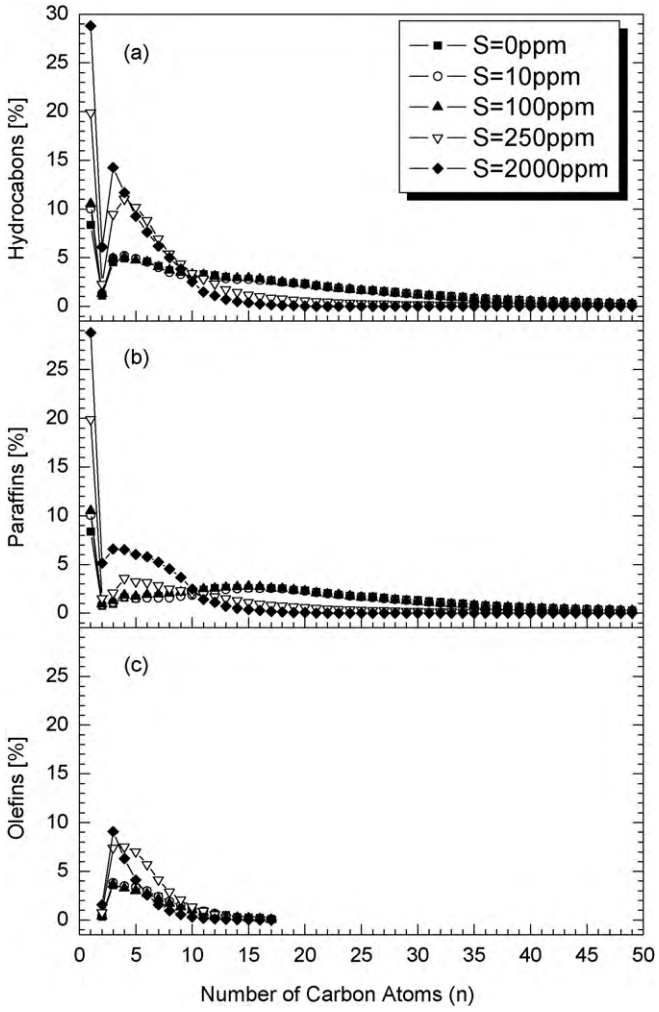

Fig. 1. Process selectivity in terms of (a) total hydrocarbons, (b) n-paraffins and (c) α-olefins as a function of carbon atom number over the various sulphured samples (experimental conditions: catalyst load 3 g, diluted 1:2 (v/v) with α-Al_2O_3; T_{cat} = 493 K; P = 20 bar; H_2/CO inlet molar ratio = 2; GHSV = 5000 $cm^3(STP)/h/g_{cat}$, sulphur amount on the catalyst = 0–2000 ppm_w).

thesis and strongly depends on the amount of sulphur loaded onto the catalyst [5].

The detailed kinetic description of the FTS in the presence of sulphided catalyst is an important feature for both the industrial practice and the comprehension of the sulphur effects on the reaction mechanism. In particular, the development of a kinetic model able to predict at the same time the reactants conversion and the products distribution (i.e. a detailed kinetic model) either in the case of fresh or partially poisoned catalyst is a prerequisite for the design, optimization, and simulation of the industrial processes fed with sulphur containing syngas. However, such a model is still lacking in the open literature to our knowledge. In order to fulfil this demand, in the present work, the mathematical description of the data reported in [5] has been extended also to products selectivity.

A complete kinetic mechanistic model for the Fischer–Tropsch synthesis over a Co/Al_2O_3 unpoisoned catalyst, able to predict simultaneously both the CO conversion and the n-paraffins and α-olefins selectivity from C_1 to C_{50} on the basis of the process conditions, had been reported by some of us in [13–15]. A fundamental approach was followed to develop this model. First, a detailed FTS mechanism for a cobalt-based catalyst was defined, explaining the synthesis of each product through the evolution of reaction intermediates and adsorbed species. Then, appropriate rate laws were attributed to each elementary step. Finally, the resulting kinetic scheme was fitted to a comprehensive set of FTS runs.

In the present work we have extended this model to make it suitable to describe also the performances of partially deactivated catalysts. The developed model allows to predict simultaneously both the CO conversion and the n-paraffins and α-olefins selectivity up to $n = 50$, on the basis of the process conditions and the sulphur loading on the catalyst surface.

2. Kinetic modeling

In the following, the kinetic model developed in [13–15] to describe the activity of the unpoisoned catalyst, and modified in this work to introduce the effects of sulphur poisoning on the performances of the adopted catalyst, will be briefly recalled.

2.1. The reaction scheme

The unassisted CO dissociation version of the carbide theory [16,17] has been adopted to describe CO conversion, while the alkyl mechanism [18] has been adopted to describe the chain growth process. Accordingly, the FT reaction pattern has been detailed as follows [13–15]:

$$\text{Step1}: \quad H_2 + 2* \leftrightarrows 2H* \tag{3}$$

$$\text{Step2}: \quad CO + * \leftrightarrows CO* \tag{4}$$

$$\text{Step3}: \quad CO* + * \rightarrow C* + O* \tag{5}$$

$$\text{Step4}: \quad C* + H* \rightarrow CH* + * \tag{6}$$

$$\text{Step5}: \quad CH* + H* \rightarrow CH_2* + * \tag{7}$$

$$\text{Step6}: \quad O* + H* \rightarrow OH* + * \tag{8}$$

$$\text{Step7}: \quad OH* + H* \rightarrow H_2O + 2* \tag{9}$$

$$\text{Step8}: \quad CH_2* + H* \rightarrow CH_3* + * \tag{10}$$

$$\text{Step9}: \quad R_n* + CH_2* \rightarrow R_{n+1}* + *, \quad n: 1 \rightarrow \text{NP-1} \tag{11}$$

$$\text{Step10}: \quad CH_3* + H* \rightarrow CH_4 + 2* \tag{12}$$

$$\text{Step11}: \quad R_n* + H* \rightarrow P_n + 2*, \quad n: 2 \rightarrow \text{NP} \tag{13}$$

$$\text{Step12}: \quad C_2H_5* \leftrightarrows C_2H_4 + H* \tag{14}$$

$$\text{Step13}: \quad R_n* \leftrightarrows O_n + H*, \quad n: 3 \rightarrow \text{NP} \tag{15}$$

where P_n and O_n are the generic linear paraffin and α-olefin with n carbon atoms, respectively, and $R_n{}^*$ is the generic growing adsorbed linear hydrocarbon species (with the generic formula ${}^*CH_2(CH_2)_{n-1}H$, with $n = 1 \rightarrow$ NP).

In the proposed mechanism, gas phase H_2 dissociates reversibly on two different free catalytic sites (*) (step 1), while gas phase CO is first adsorbed reversibly in the molecular state (step 2), then dissociates (step 3). Also the formation of the monomeric species $CH_2{}^*$ (in accordance with the carbide theory [16,17]) occurs via two steps in series – the reaction between the carbide and the surface hydrogen to form the species CH* (step 4) and the reaction between this species and the surface hydrogen to form the monomer $CH_2{}^*$ (step 5) – and the same happens to the adsorbed oxygen atom formed from the CO* dissociation (step 3), that is first hydrogenated to OH* (step 6) and then removed as water (step 7).

In accordance with the alkyl theory [18], the chain growth reaction is initiated by the formation of a methyl species (step 8) and the propagation takes places by the successive insertion of methylene into the active site-alkyl bond (step 9). Termination is the result of two different routes: a dual-site reaction between the intermediate $R_n{}^*$ and an adsorbed hydrogen atom (steps 10 and 11) giving n-paraffins or a reversible β-hydride elimination reaction (steps 12 and 13) giving α-olefins.

2.2. The kinetic model

An elementary rate law or an equilibrium constant has been assigned to each step involved in the detailed reaction mechanism of FTS. Accordingly, the FT kinetics has been detailed as follows [13–15]:

$$\text{Step 1}: \quad K_{eq_{H_2}} = \vartheta_{H^*}^2 P_{H_2}^{-1} \vartheta^{-2} \tag{16}$$

$$\text{Step 2}: \quad K_{eq_{CO}} = \vartheta_{CO^*} P_{CO}^{-1} \vartheta^{-1} \tag{17}$$

$$\text{Steps 3} - 7: \quad r_M = k_M \vartheta_{CO^*} \vartheta \tag{18}$$

$$\text{Step 8}: \quad r_{IN} = k_{IN} \vartheta_{CH_2{}^*} \vartheta_{H^*} \tag{19}$$

$$\text{Step 9}: \quad r_{G,n} = k_G \vartheta_{R_n{}^*} \vartheta_{CH_2{}^*} \tag{20}$$

$$\text{Step 10}: \quad r_{CH_4} = k_{CH_4} \vartheta_{CH_3{}^*} \vartheta_{H^*} \tag{21}$$

$$\text{Step 11}: \quad r_{P,n} = k_P \vartheta_{R_n{}^*} \vartheta_{H^*} \tag{22}$$

$$\text{Step 12}: \quad r_{C_2H_4} = \vec{r}_{O,2} - \overleftarrow{r}_{C_2H_4} = k_{O,dx} \vartheta_{C_2H_5{}^*} - k_{C_2H_4} x_{C_2H_4} \vartheta_{H^*} \tag{23}$$

$$\text{Step 13}: \quad r_{O,n} = \vec{r}_{O,n} - \overleftarrow{r}_{O,n} = k_{O,dx} \vartheta_{R_n{}^*} - k_{O,sx} x_{O_n} \vartheta_{H^*} \tag{24}$$

where ϑ is the fraction of free catalytic sites, ϑ_i is the fraction of the catalytic sites occupied by species i and x_{O_n} is the molar fraction of the α-olefin with n carbon atoms in the liquid phase surrounding the catalyst pellets.

Both the H_2 dissociative adsorption (step 1) and the CO molecular adsorption (step 2) have been assumed to approach equilibrium at the actual process conditions [14,15]. For this reason two equilibrium constants (Eqs. (16) and (17)) have been assigned to these steps. In contrast, for steps 3–7 we have assumed that CO* dissociation (step 3) is rate determining in these sequence of consecutive, non-reversible and kinetically controlled steps that lead to the formation of methylene species and water [14,15]. Accordingly, the overall rate of all such steps has been described by the rate expression for CO dissociation (Eq. (18)).

It has been also assumed that the rate constants describing the elementary steps for the growth of the adsorbed species $R_n{}^*$ (step 9), the formation of the paraffins C_{2+} (step 11) and the formation of the olefins C_{3+} (step 13) are independent of the carbon atom number of the intermediates involved in the elementary reactions [13–15].

In order to describe the experimental deviation of methane and ethylene from Anderson–Schulz–Flory (ASF) product distribution, specificity has been assumed in the kinetic constants involved in the kinetic expressions for the formation of these species (steps 10 and 12) [13–15].

On the basis of the experimental observation that the reaction temperature strongly affects CO conversion and the hydrogenation reactions (and hence the olefin/paraffin ratio) while the effect on the chain growth probability is weak, only rate expressions (18), (21) and (22) have been considered as activated [14,15]. In this way, CO and H_2 heats of adsorption are lumped in the activation energy calculated for steps 3–7, 10 and 11. According to the Arrhenius law, the kinetic constants involved in the temperature-activated steps have been written as:

$$k_M = k_M^0 \exp\left(-\frac{E_M}{RT}\right) \quad (25)$$

$$k_{CH_4} = k_{CH_4}^0 \exp\left(-\frac{E_{CH_4}}{RT}\right) \quad (26)$$

$$k_P = k_P^0 \exp\left(-\frac{E_P}{RT}\right) \quad (27)$$

where k_i^0 is the pre-exponential factor and E_i the activation energy referred to the kinetic constant k_i.

The molar fraction of the α-olefin with n carbon atoms in the liquid phase surrounding the catalyst pellets (x_{O_n}) has been evaluated by means of an explicit correlation, expressing dependence of this parameter on temperature, number of carbon atoms and partial pressure of the corresponding olefin in the gas phase, obtained on the basis of a priori vapor–liquid equilibrium calculation using the Soave–Redlich–Kwong cubic equation of state. This introduces an implicit dependence of the chain growth probability on the chain length, resulting from higher solubilities of olefins with higher carbon atom numbers.

2.3. The effect of sulphur on the FT kinetics

From the data reported in Table 1 in terms of CO conversion, early discussed in Section 1, it is evident that the activity of the catalyst is greatly decreased by sulphur and that this effect is strong already at very low poison loadings. As a matter of facts, while the residual activity of the sample loaded with 10 ppm_w of sulphur is less than 80% of the activity of the unpoisoned catalysts, the activity of the most sulphided catalyst we tested, loaded with 2000 ppm_w, is almost nil. This effect was explained in [5] considering the ability of sulphur both to prevent the complete reduction of cobalt oxides during the catalyst activation treatment, thus inhibiting the formation of the active sites, and to poison selectively part of the active sites available on the catalyst surface.

In order to fit the CO conversion decrease upon increasing the sulphur content on the catalyst, the number of available catalytic sites (nacs) on the surface of the poisoned catalysts has been described in the kinetic model according to the following equation:

$$\text{nacs} = \frac{\text{nacs}^0}{(1+\alpha_{\text{sites}}S)^{m_{\text{sites}}}} \quad (28)$$

where nacs^0 is the number of available catalytic sites on the unpoisoned catalyst (named S0 in [5]), S the sulphur content on the catalyst expressed in mg_S/kg_{cat} and α_{sites}, m_{sites} two positive adaptive parameters. The structure of Eq. (28) has been chosen in order to reflect that of Eq. (2), that is the best deactivation model found in [5] to describe the CO conversion trend upon changing the sulphur content on the catalyst.

In terms of process selectivity, calculated as the ratio between the molar productivity of each species multiplied by its number of carbon atoms (carbon productivity) and the total carbon productivity of the products, Fig. 1 shows that the presence of sulphur on the catalyst surface induces a strong decrease of the selectivity to the high molecular weight products both in the case of paraffins and in the case of olefins. In our previous work [5], this effect was tentatively ascribed to the ability of sulphur to poison the (ensemble) sites required to catalyse the chain growth process (step 9). Due to the polymerization nature of the Fischer–Tropsch synthesis, in fact, the rate of the chain growth process (propagation step) is directly responsible for the average molecular weight of the reaction products: upon increasing the chain growth process the selectivity to heavy products is increased and vice versa.

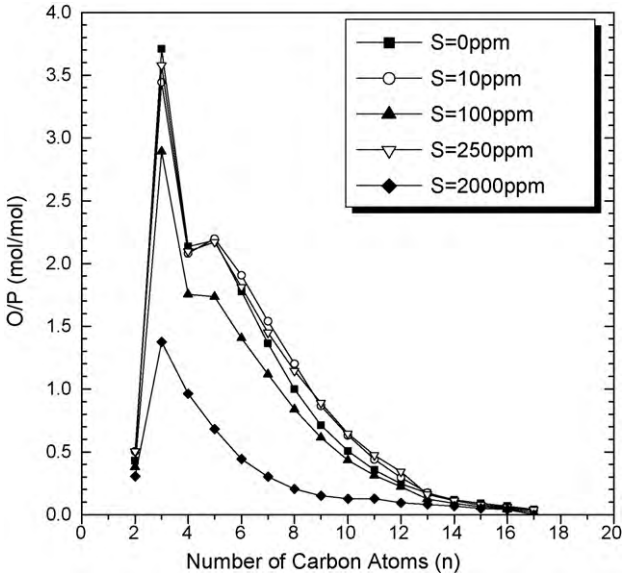

Fig. 2. Experimental olefin to paraffin ratio (O/P) as a function of the number of carbon atoms in the products (n) for samples loaded with different amounts of sulphur (experimental conditions as in Fig. 1).

Starting from the experimental observation that sulphur loadings lower than 100 ppm_w do not significantly affect the selectivity of the FTS, while the selectivity of the process is rapidly shifted to low molecular weight products at higher sulphur contents [5], for the catalyst samples loaded with sulphur amounts higher than 100 ppm_w, we have introduced the dependence on sulphur content in the kinetic expression associated with the chain growth reactions (Eq. (20)). In particular, the rate r_G was expressed as:

$$r_{G,n} = r_{G,n}^0 \quad \text{if } S \le 100\ ppm_w \quad (29)$$

$$r_{G,n} = \frac{r_{G,n}^0}{(1+\alpha_G(S-100))^{m_G}} \quad \text{if } S > 100\ ppm_w \quad (30)$$

where $r_{G,n}^0$ is the chain growth rate of the unpoisoned catalyst and α_G, m_G two positive adaptive parameters.

In Fig. 2, the experimental values of the olefin to paraffin ratio in the products are reported both in the case of unpoisoned and in the case of poisoned catalyst samples. It is evident that the presence of sulphur decreases this ratio, in particular for the most sulphided catalyst we tested. In order to describe this effect, the rates of both paraffins and olefins formation (Eqs. (11) and (13), respectively) have been expressed as a function of sulphur amount on the catalysts, according to the following expressions:

$$r_{P,n} = r_{P,n}^0(1+\alpha_{P,n}S) \quad (31)$$

$$r_{O,n} = \vec{r}_{O,n}^0 - \tilde{r}_{O,n}^0(1+\alpha_{O,n}S) \quad (32)$$

where $r_{P,n}^0$, $\vec{r}_{O,n}^0$ and $\tilde{r}_{O,n}^0$ are the rates of paraffins formation, olefins desorption and olefins readsorption for the unpoisoned cat-

alyst, respectively, and $\alpha_{P,n}$, $\alpha_{O,n}$ two positive adaptive parameters.

The structure of Eq. (31) has been chosen to express the enhanced hydrogenating activity of the poisoned catalysts, which in our opinion is one of the reasons of the decreased olefin/paraffin ratio in the products collected during runs over the poisoned catalysts.

The introduction of an effect of sulphur in the olefin readsorption rate ($\tilde{r}_{O,n}$, Eq. (32)), on the contrary, has to be considered an indirect way to correct the explicit correlation we used to compute the molar fraction of each olefin in the liquid phase surrounding the catalyst pellets at the reaction conditions (see Eq. (24)). This correlation, in fact, was developed considering the typical composition of the liquid phase trickling in the FT fixed-bed reactors, working with unpoisoned catalysts; however, in the presence of sulphur-poisoned catalysts, due to the significant decrease of the chain growth probability, we expect to have a liquid phase lighter than usual, in which the solubility of the (light) olefins, and thus their readsorption rate, is higher.

Along similar lines, considering the anomalous behaviour of ethylene, already discussed in Section 2.2, a specific law has been used to describe the effect of sulphur on the readsorption rate of this species:

$$r_{C_2H_4} = \vec{r}^{0}_{O,2} - \tilde{r}^{0}_{C_2H_4}(1+\alpha_{O,2}S)^{m_{O,2}}$$

where $\tilde{r}^{0}_{C_2H_4}$ is the rate of ethylene readsorption for the unpoisoned catalyst, and $\alpha_{O,2}$, $m_{O,2}$ two positive adaptive parameters.

2.4. The reactor model

The reactor model adopted for describing the lab-scale fixed-bed reactor used to collect the activity data of both the unpoisoned [13–15] and the poisoned [5] catalysts is an isothermal heterogeneous plug-flow model. It is composed by:

- 2NP + 2 ordinary differential equations (33), expressing the material balances for both the reactants (CO, H_2) and the products (H_2O, linear paraffins $C_1 \rightarrow C_{NP}$, olefins $C_2 \rightarrow C_{NP}$) of the reaction;
- 2NP + 2 initial condition (34) for the differential equations (33), assigning the value of flow of each species at the reactor inlet ($W_{cat} = 0$);
- NP + 3 algebraic equations of the type (35), expressing the material balances for the adsorbed species (H^*, CO^*, $CH_2{}^*$, $R_n^{*\,n:1\rightarrow NP}$);
- the catalytic sites balance (36).

$$\frac{dF_i}{dW_{cat}} = \sum_{k=1}^{NR}\alpha_{i,k}r_k \tag{33}$$

$$W_{cat} = 0 \quad F_i = F_{i,0} \tag{34}$$

$$0 = \sum_{k=1}^{NR}\alpha_{j,k}r_k \tag{35}$$

$$1 = \theta + \theta_{H^*} + \theta_{CO^*} + \theta_{CH_2^*} + \sum_{n=1}^{NP}\theta_{R_n^*} \tag{36}$$

where F_i and $F_{i,0}$ are the molar flows of the generic species i (i = CO, H_2, H_2O, CH_4, $P_n^{n:2\rightarrow NP}$, C_2H_4, $O_n^{n:3\rightarrow NP}$) along the reactor axis and at the reactor inlet, respectively, W_{cat} the catalyst mass, $\alpha_{i,k}$ and $\alpha_{j,k}$ the stoichiometric coefficients for the ith and for the jth (j = H^*, CO^*, $CH_2{}^*$, $R_n^{*n:1\rightarrow NP}$) species, respectively, in the kth reaction, r_k the rate of the kth reaction and NR the number of the elementary steps (or group of elementary steps if described with the same rate expression) involved in the process.

Table 2
Estimates of the 8 adaptive parameters involved in the deactivation expressions used for the description of the reactivity of the poisoned catalyst samples.

Parameter	Estimate	Unit
α_{sites}	9.0×10^{-2}	ppm^{-1}
m_{sites}	2.5×10^{-1}	–
α_G	6.0×10^{-1}	ppm^{-1}
m_G	3.0×10^{-1}	–
$\alpha_{P,n}$	6.0×10^{-4}	ppm^{-1}
$\alpha_{O,n}$	6.0×10^{-4}	ppm^{-1}
$\alpha_{O,2}$	1.5×10^{-1}	ppm^{-1}
$m_{O,2}$	2.5×10^{-1}	–

2.5. Optimization method

In order to obtain the best fit of the 47 experimental data-set collected over the unpoisoned catalyst (46 experiments described in Refs. [13–15], 1 experiment described in Ref. [5]) we adopted 13 kinetic/thermodynamic adaptive parameters ($K_{eq_{H_2}}$, $K_{eq_{CO}}$, k_M, k_{IN}, k_G, k_P, k_{CH_4}, $k_{O,dx}$, $k_{O,sx}$, $k_{C_2H_4}$, E_M, E_P, E_{CH_4}). Other 8 empirical adaptive parameters (α_{sites}, m_{sites}, α_G, m_G, α_{P_n}, $\alpha_{O,2}$, $m_{O,2}$, $\alpha_{O,n}$) were added to describe the effect of sulphur on the performances of the adopted catalyst, experimentally investigated at steady state conditions with catalysts loaded with 5 different sulphur amounts [5].

The 13 kinetic/thermodynamic parameters referred to the unpoisoned catalyst were estimated in [13–15] by a non-linear multi-response regression, performed using the Fortran subroutine BURENL [19] based on the least-squares method. The algebraic-differential system constituted by Eqs. (33), (35) and (36) was integrated numerically with the Fortran subroutine LSODI [20], that allows to solve stiff problems using Gear's implicit integration method with variable step. The regression was performed using as experimental responses the CO conversion and the CH_4, C_2H_4, C_2H_6, C_3H_6, C_3H_8, C_6H_{12}, C_6H_{14}, $C_{10}H_{20}$, $C_{10}H_{22}$, $C_{12}H_{26}$, $C_{15}H_{32}$, $C_{20}H_{42}$, $C_{25}H_{52}$, $C_{30}H_{62}$, $C_{35}H_{72}$, $C_{45}H_{92}$, C_{5+} and olefins selectivity.

The 8 empirical parameters referred to the unpoisoned catalyst were separately estimated in this work, following the same approach.

2.6. Model fit

In our previous works [14,15], the ability of the developed model to describe the effect of the process conditions on both the CO conversion and the products distribution was shown in the case of the unpoisoned catalyst. In this work, those results, which are still valid for the unpoisoned catalyst, will not be reported anymore; on the contrary, the ability of the model to describe the sulphur effects on both the catalyst activity and selectivity will be shown and discussed.

The estimates of the 8 adaptive parameters used to describe the effects of sulphur on the reactivity of the adopted catalytic system and estimated upon regression of the experimental data-set described in Ref. [5] are listed in Table 2. The presence of sulphur decreases both the number of the active sites and their activity in the chain growth process. In the case of the active sites number, this effect is very strong already at very low sulphur poisoning, so that the number of residual active sites is about 85% at 10 ppm_w and is more then halved at 170 ppm_w. In the case of the chain growth rate, the poisoning effect is even stronger than in the case of the loss of activity, but the deactivation is "delayed" and begins, as discussed in Section 2.3, for sulphur loadings greater than 100 ppm_w.

On the contrary, sulphur poisoning increases linearly the rate of paraffins formation, so that in the case of the sample loaded with 2000 ppm_w the rate of formation of these species from the

growing intermediate R_n^* is more than doubled with respect to the unpoisoned sample.

Also, as expected, the presence of sulphur increases the rate of olefins readsorption, as a consequence of their higher solubility in the liquid phase surrounding the catalyst pellets packed in the reactor. This effect is particularly evident in the case of ethylene, possibly as a consequence of the fact that this is the olefin with the lowest solubility and the higher diffusivity in the waxes.

The ability of the model to describe the CO conversion trend at fixed process conditions, upon changing the sulphur loading on the catalyst, is shown in Fig. 3. The model can satisfactorily predict all the collected experimental data: the average relative error is 16%, a satisfactory value which is comparable to those obtained in our previous works with the unpoisoned catalyst [14,15].

In Fig. 4(a)–(d), the experimental and calculated selectivities to the main reaction products are reported. In the case of methane (Fig. 4(a)) and ethylene (Fig. 4(b)), the model nicely fits the increase of the selectivity with increasing the sulphur loading. The same happens for the decreasing trend shown by the selectivity to C_{5+} hydrocarbons (Fig. 4(c)). It is worth noticing that the model correctly describes both the unchanged selectivity to these species for sulphur loadings up to 100 ppm and the growing/decreasing trends for higher poison contents. The olefin selectivity is shown in Fig. 4(d) as a function of the sulphur content on the catalyst. Again, the model correctly fits the experimental data, accounting for the high selectivity to unsaturated hydrocarbons experimentally observed running the catalyst sample loaded with 250 ppm_w of sulphur. As discussed in [5], this may be associated with the observed (and modeled) changes in the product distribution upon sulphur addition, i.e. the decrease of the selectivity to heavy products, which contain only paraffins, and the increase of the hydrogenating activity of the catalyst. Indeed, while the former effect would increase the olefinicity of the products, the latter would decrease it, resulting in a non-monotonic trend of the olefin selectivity as a function of the sulphur loading on the catalyst.

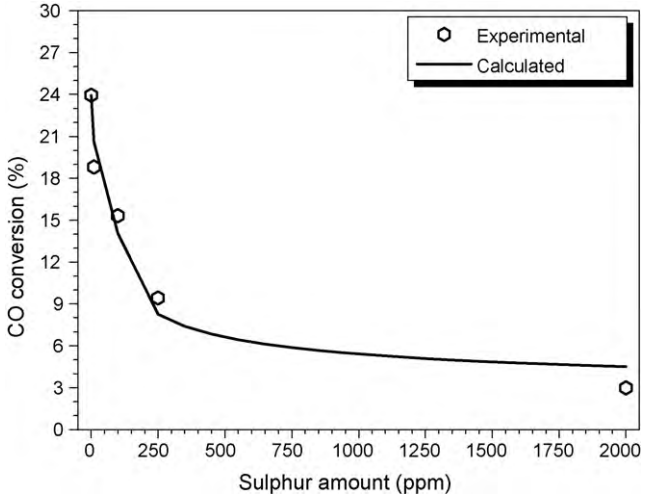

Fig. 3. Experimental and calculated CO conversion for samples loaded with different amounts of sulphur (experimental conditions as in Fig. 1). Experimental data are taken from Ref. [5].

In terms of ASF product distribution, in our previous works [14,15] we showed that the developed model is able to satisfactorily describe the product selectivity, accounting for the typical deviations of the product distribution from the ASF model, namely

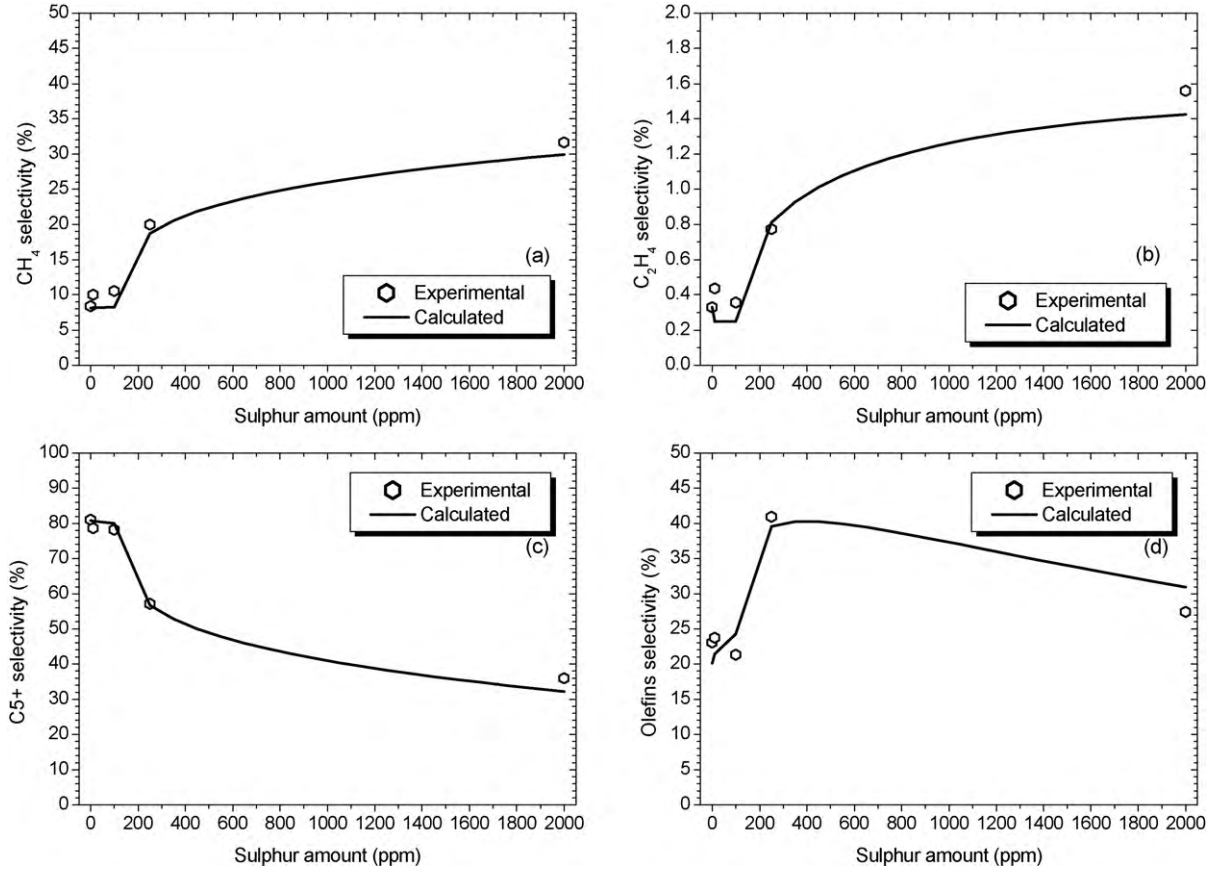

Fig. 4. Experimental and calculated selectivities to the main reaction products for samples loaded with different amounts of sulphur: (a) CH_4, (b) C_2H_4, (c) C_{5+} and (d) olefins (experimental conditions as in Fig. 1). Experimental data in plots (a), (c) and (d) are taken from Ref. [5].

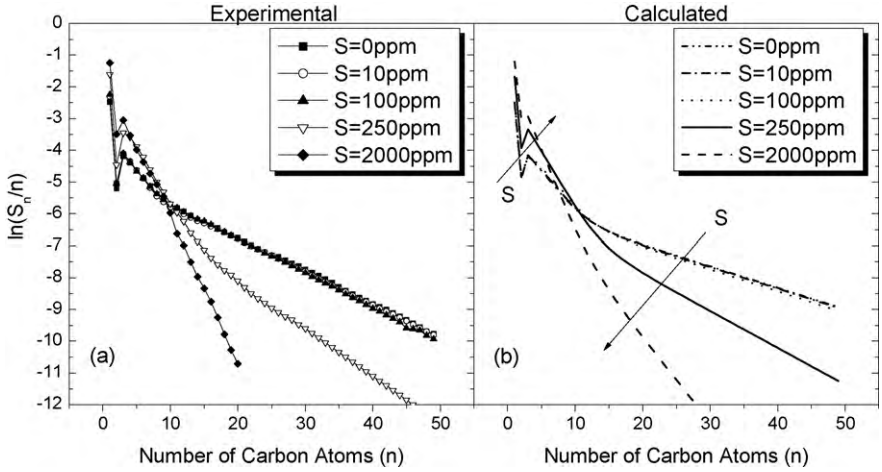

Fig. 5. Total hydrocarbons (a) experimental and (b) calculated ASF distributions reported in terms of carbon selectivity (S_n) for samples loaded with different amounts of sulphur (experimental conditions as in Fig. 1). Experimental data are taken from Ref. [5].

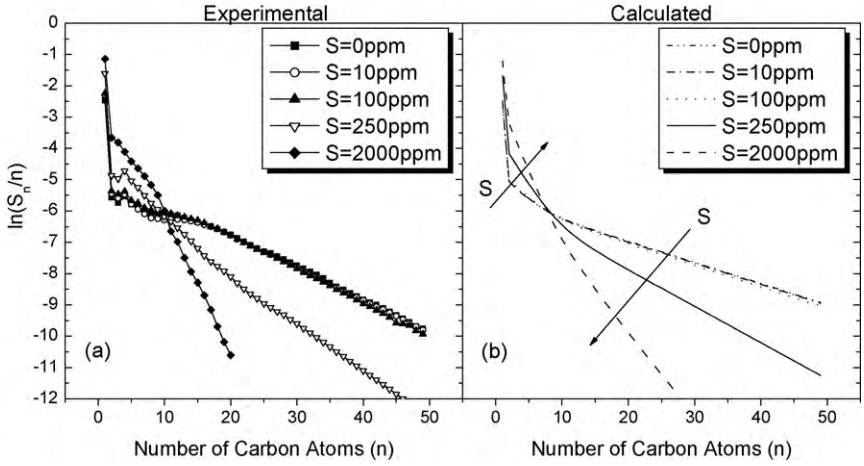

Fig. 6. Paraffins (a) experimental and (b) calculated ASF plots reported in terms of carbon selectivity (S_n) for samples loaded with different amounts of sulphur (experimental conditions as in Fig. 1).

the high methane selectivity, the low selectivity to ethylene and the change of the ASF slope with growing carbon atoms number. Also, we showed that the developed model is able to correctly describe the effects of all the investigated process conditions (temperature, pressure, H_2/CO inlet ratio and gas hourly space velocity) on the products distributions with a single set of rate parameter estimates.

The model fits of the ASF products distributions in terms of total hydrocarbons, paraffins and olefins for the samples loaded with

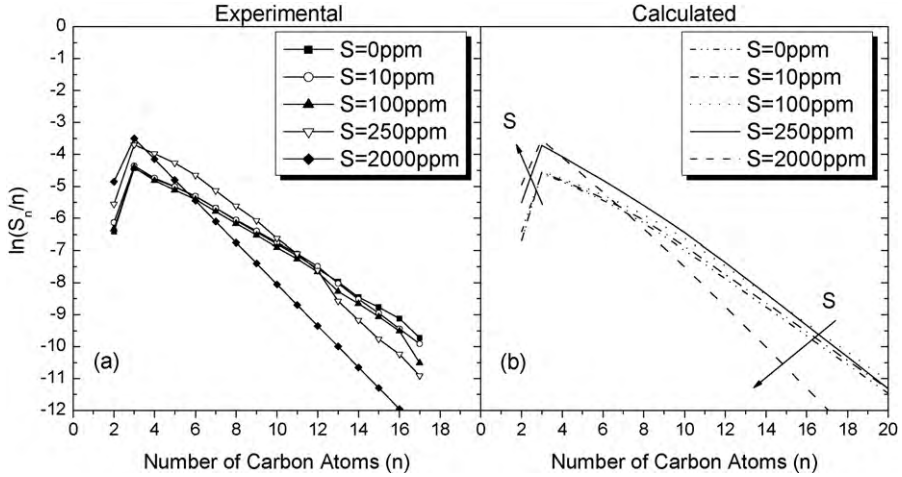

Fig. 7. Olefins (a) experimental and (b) calculated ASF plots reported in terms of carbon selectivity (S_n) for samples loaded with different amounts of sulphur (experimental conditions as in Fig. 1).

different amounts of sulphur are shown in Figs. 5–7. Thanks to a single set of the 8 adaptive empirical parameters introduced in the kinetic scheme in this work, the "modified" model nicely fits also the variation of the ASF distribution upon increasing the sulphur loading, accounting both for the increase of the selectivity of the light species and for the decrease of the selectivity to the heavy products for sulphur loading greater than 100 ppm_w.

3. Conclusions

The complete kinetic model of FTS over a Co/Al_2O_3 un-promoted catalyst developed in [14,15] for a fresh unpoisoned catalyst has been extended in this work in order to make it able to describe also the activity and the selectivity of a sulphur-poisoned catalyst, loaded with sulphur loads between 0 and 2000 ppm_w.

This result has been achieved by selectively introducing in the original model 8 additional adaptive parameters. More specifically, these parameters have been used to account for the effects of sulphur (i) in decreasing the number of the active sites on the catalyst surface, that in turn induces the decrease of both the reactants conversion and the products yields, (ii) in decreasing the chain growth process rate, with the consequential decrease of the chain growth probability and the shift of the process selectivity towards the lightest reaction products, (iii) in increasing the hydrogenating ability of the catalyst, with the consequent decrease of the olefinicity of the products, and (iv) in increasing the olefins readsorption rate.

For the range of industrially relevant conditions (temperature = 210–235 °C, pressure = 8–25 bar, H_2/CO inlet molar ratio = 1.7–2.3, gas hourly space velocity = 4000–7000 $cm^3(STP)/h/g_{cat}$, sulphur loading on the catalyst = 0–2000 ppm_w) the developed model can accurately predict both the observed CO conversion and the products distribution up to $n = 50$, in terms of total hydrocarbons, n-paraffins and α-olefins. In particular, using a single set of 13 + 8 parameters, the model is able to describe the effects of the process conditions on the products yields, well accounting for the typical deviations of the products distribution from the ASF model, i.e. the methane high selectivity, the low selectivity to C_2 species and the change of the slope of the ASF plot with growing carbon number. Accordingly, the present model can be applied to predict the modification of the performances of the adopted catalyst due to the sulphur poisoning both in terms of catalyst activity and selectivity.

References

[1] E. Iglesia, Appl. Catal. A: Gen. 161 (1997) 59–78.
[2] A. Jess, R. Popp, K. Hedden, Appl. Catal. A 186 (1999) 321–342.
[3] S.T. Sie, M.M.G. Senden, H.M.H. van Wechem, Catal. Today 8 (1991) 371–394.
[4] M.E. Dry, Catal. Today 71 (2002) 227–241.
[5] C.G. Visconti, L. Lietti, P. Forzatti, R. Zennaro, Appl. Catal. A: Gen. 330 (2007) 49–56.
[6] H.G. Stenger, C.N. Satterfield, Ind. Eng. Chem. Proc. DD 24 (1985) 415–420.
[7] Z.T. Liu, J.L. Zhou, B.J. Zhang, J. Mol. Catal. 94 (1994) 255–261.
[8] C.H. Bartholomew, R.M. Bowman, Appl. Catal. 15 (1985) 59–67.
[9] T.C. Bromfield, N.J. Coville, Appl. Catal. 186 (1999) 297–307.
[10] Z.T. Liu, Y.W. Li, J.L. Zhou, Z.X. Zhang, B.J. Zhang, Appl. Catal. 161 (1997) 137–151.
[11] J. Li, N.J. Coville, Appl. Catal. 208 (2001) 177–184.
[12] R. Zennaro, M. Tagliabue, C.H. Bartholomew, Catal. Today 58 (2000) 309–319.
[13] C.G. Visconti, E. Tronconi, L. Lietti, R. Zennaro, P. Forzatti, Chem. Eng. Sci. 62 (2007) 5338–5343.
[14] C.G. Visconti, Z. Ballova, E. Tronconi, L. Lietti, R. Zennaro, P. Forzatti, Prepr. Pap. – Am. Chem. Soc. Div. Pet. Chem. 53 (2) (2008) 91–95.
[15] C.G. Visconti, Z. Ballova, L. Lietti, E. Tronconi, R. Zennaro, P. Forzatti, in: B.H. Davis, M.L. Occelli (Eds.), Advances in Fischer–Tropsch Synthesis, Catalysts and Catalysis, CRC Press, Boca Raton, 2009, pp. 293–315.
[16] F. Fischer, H. Tropsch, Berichte der Deutschen Chemischen Gesellschaft 59 (1926) 830–831.
[17] P.M. Maitlis, Pure Appl. Chem. 61 (1989) 1747–1754.
[18] R.C. Brady, R. Pettit, J. Am. Chem. Soc. 102 (1980) 6181–6182.
[19] G. Buzzi-Ferraris, G. Donati, Chem. Eng. Sci. 29 (1974) 1504–1509.
[20] A.C. Hindmarsh, in: R.S. Stepleman, M. Carver, R. Peskin, W.F. Ames, R. Vichnevetsky (Eds.), Scientific Computing, North-Holland Publishing Company, Amsterdam, 1983, pp. 55–64.